Mode Coarsening or Fracture: Energy Transfer Mechanisms in Dynamic Buckling of Rods

E. Villermaux,[1,2,3] K. Keremidis,[4] N. Vandenberghe,[2] M. J. Abdolhosseini Qomi,[5] and F.-J. Ulm[1,4,*]

[1]MIT-CNRS Joint Lab "Multiscale Materials Science for Energy and the Environment," Massachusetts Institute of Technology, Cambridge, Massachusetts 02139, USA

[2]Aix Marseille Université, CNRS Centrale Marseille, IRPHE, 13013 Marseille, France

[3]Institut Universitaire de France

[4]Department of Civil and Environmental Engineering, Massachusetts Institute of Technology, Cambridge, Massachusetts 02139, USA

[5]Department of Civil and Environmental Engineering, University of California Irvine, Irvine, California 92697, USA

(Received 17 June 2020; accepted 23 December 2020; published 27 January 2021)

We present results of a hybrid experimental, theoretical, and simulation-based investigation of the postbuckling behavior of thin elastic rods axially impacted by a projectile. We find a new postbuckling mechanism: mode coarsening. Much akin to inverse energy cascade phenomena in other nonlinear dynamic systems, energy is transferred during mode coarsening from higher to lower wave numbers—unless the rod breaks, abruptly dissipating in the course of fracture the rod's strain energy. We derive a model that provides a predictive means to capture mode coarsening in the form of a nondissipative, purely geometric force relaxation mechanism, and validate the model by means of molecular dynamics (MD) based structural dynamics simulations for rods of wood and pasta considering different thermodynamic ensembles. The scalability of theory and simulation for engineering applications opens new venues toward safe design of engineering structures subject to impact-induced risks of buckling, ranging from skyscrapers, to aerospace structures, to the crashworthiness of vehicles, for example.

DOI: 10.1103/PhysRevLett.126.045501

Buckling, that is the elastic instability of rods subject to compression loads, is one of the most studied phenomena in engineering mechanics, ever since Euler in 1744 derived the critical buckling load beyond which an initial straight rod exhibits excessive lateral bending deflection [1]. This continuous scholarly interest owes much to the importance of buckling in many engineering applications ranging from civil and mechanical engineering [2,3] and thin aerospace structures [4], to protein microtube buckling in biomechanics applications [5]. Beside the omnipresence in application, much emphasis has been given to understanding the development and propagation of instabilities in dynamic buckling which occur when the load is applied suddenly, as during impact [6–8] or stress release [9,10]. In fact, following an impact, the preferred wavelength of the buckling instability of rods (Fig. 1) is quite different from Euler's *static* buckling mode, and drives characteristic fragmentation patterns of brittle rods [11], or the time-dependent wrinkling pattern of impacted sheets [12,13]. Yet, a wealth of questions remains when it comes to purely elastic dynamic buckling; that is, when no energy is dissipated by small scale thermal fluctuations [14], long-range viscous deformation [2], or abrupt fracture.

Here, we focus on the postbuckling behavior of thin elastic rods subject to sudden impact and approach this problem through a combination of experiments, first-order analytical solutions, and molecular dynamics (MD) based simulations of buckling tests in different thermodynamic ensembles. Through this combination we show that, after impact, a time-dependent geometric relaxation phenomenon takes place, during which energy is transferred from higher to lower wave numbers [Figs. 1(a1)–1(e1)]; unless the rod breaks [Figs. 1(a2)–1(e2)], dissipating in the course of fracture the rod's strain energy and leading to an abrupt force relaxation. Such competition between force relaxation and fragmentation during instability development seems to be a general pattern of many deformable systems, including the dynamical fragmentation of membranes [15].

Our typical experimental setup for dynamic buckling consists of a projectile axially impacting two types of rods clamped on the nonimpacted side, as shown in Fig. 1: an elastic rod made of wood ($\rho = 0.5$ g/cm^3, rectangular cross section of width $b = 3.1$ mm, thickness $d = 0.53$ mm, and length $\ell = 720$ mm with Young's modulus $E = 10$ GPa); and a brittle rod made of dry pasta ($\rho = 1.5$ g/cm^3, circular cross section of diameter $d = 0.8$ mm, and length $\ell = 250$ mm with Young's modulus $E = 3$ GPa). The steel cylindrical projectile (14.6 mm diameter, mass 10 g) falls by its own weight through a long acrylic tube from a given height adjusted to reach the desired impact velocity U_0. The impact dynamics, deformation, and possible fragmentation of the rod are recorded at a rate of the order of 10^5 frames per second. Impact results in a transient longitudinal load along the rod. Instability induces the relaxation of this force.

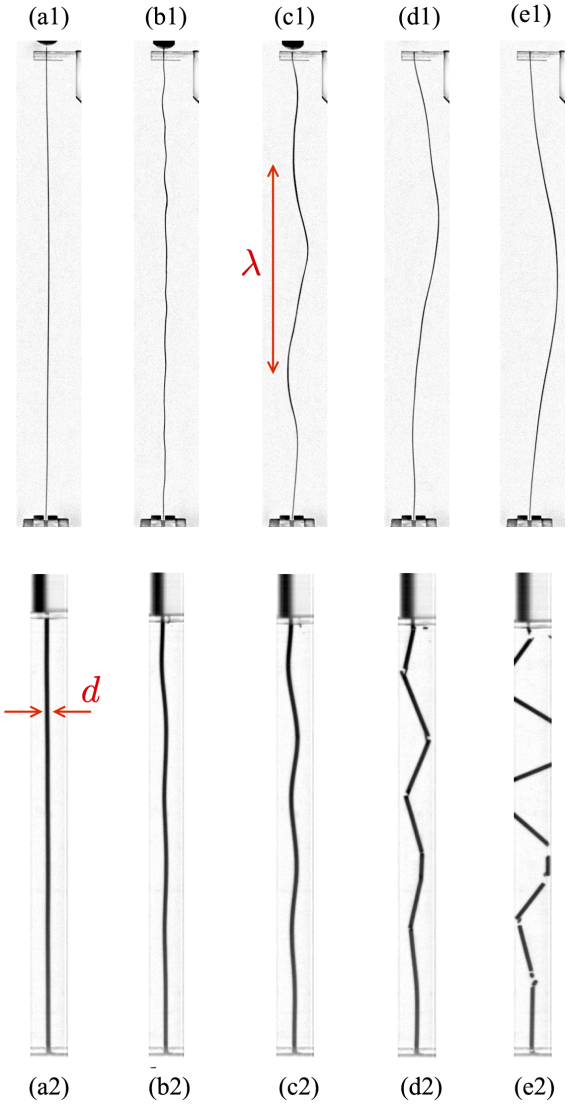

FIG. 1. Dynamic buckling experiments with (top) wooden rod (length 720 mm); (bottom) dry pasta rod (length 250 mm): (a1)–(e1) instability formation and visible mode coarsening after impact at times $t/\tau = 0$, 2.5, 45, 149, 300 (buckling time $\tau = d/U_0 \approx 2 \times 10^{-4}$ s, with $U_0 = 2.72$ m/s). (a2)–(e2) Instability development and fragmentation at times $t/\tau = 0$, 0.38, 0.58, 0.85, 1.58 ($\tau = 3.4 \times 10^{-4}$ s, with $U_0 = 2.3$ m/s).

Two types of force relaxation mechanisms are illustrated in Fig. 1: in the case of the elastic rod (wood) [Figs. 1(a1)–1(e1)], following the impact, the bending deformation due to buckling is small and dominated by short wavelengths [Figs. 1(b1) and 1(c1)]. Whereas a few tens of milliseconds later, the bending deformation has increased and is dominated by increasingly longer wavelengths [Figs. 1(d1) and 1(e1)] through a deterministic process (see Supplemental Material [16]). Things develop quite differently for the brittle rod (dry pasta) [Figs. 1(a2)–1(e2)]. Shortly after impact a sinusoidal perturbation appears [Fig. 1(b2)], and develops into a dominating wavelength of the buckling instability. As a consequence, a few tenths of milliseconds later, the pasta has buckled appreciably and begins to shatter [Fig. 1(c2)]. The pursuing fragmentation releases the bending energy and the axial forces abruptly, imparting in the course of this process angular momentum of alternating signs to the fragments which rotate and scatter.

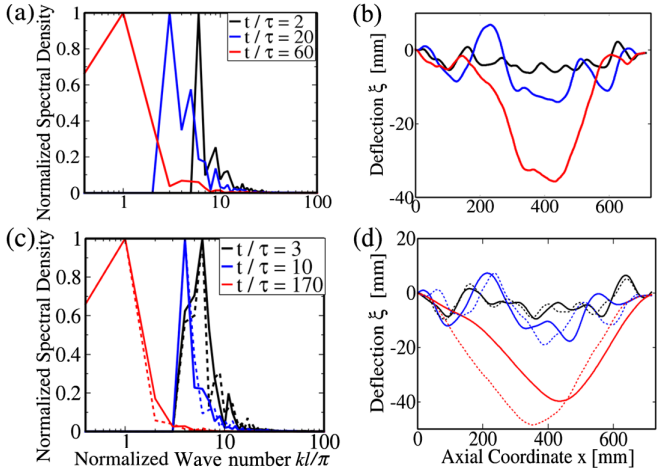

FIG. 2. Spectral density and transverse displacements for wooden rod at different time frames obtained from (a), (b) NVE simulations; and (c),(d) experiments (continuous line) and NVT simulations (dotted line) (impact duration $\tau = 2 \times 10^{-4}$ s).

We start by rationalizing these observations through a power spectral density (PSD) analysis of the deformation patterns from the beam position coordinates, $\xi_i(x)$, $i = 1, \ldots, N$, obtained from digitized images of the experiments for, respectively, $N = 5500$ time frames from the wooden rod buckling and relaxation, and $N = 700$ time frames from the dry pasta rod buckling and fragmentation. A selected number of spatial PSDs, $S_i(k)$, for the wood rod experiment are shown in Fig. 2(c), as obtained from the spatial signal $\xi_i(x)$ for a selected progression of time frames displayed in Fig. 2(d) (continuous lines). Two observations deserve attention, namely that each PSD (normalized by its maximum value) exhibits a clear peak spectral density representative of a dominating instability wave number $k = 2\pi/\lambda$ (with λ the wavelength); and that this peak spectral density shifts with time from high wave numbers (small wavelengths) to low wave numbers (long wavelengths). This time-dependent mode coarsening is displayed in Fig. 3(a) showing the dominating instability wave number versus time at which the wave number peaks in the spectral density [Fig. 2(c)]. If we remind ourselves that the spatial PSD represents (close to a multiplying factor) the energy contribution of each mode to the overall buckling bending energy, it becomes apparent that this mode coarsening in dynamic postbuckling of rods is representative of a progressive transfer of energy in time from high energy modes to low energy modes; much akin to inverse energy cascade phenomena in other nonlinear dynamic systems [17]. In contrast, the buckling of a brittle rod has no such

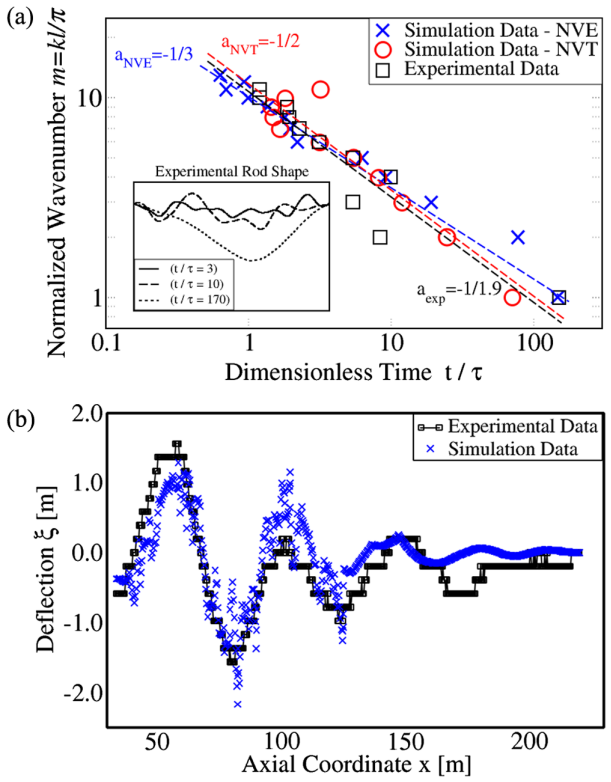

FIG. 3. Evidence of mode coarsening vs fracture competition: (a) Time of occurrence of maximum PSD vs wave number obtained, for wood rod from experiments (black), NVE simulations (blue), and NVT simulations. (b) Fragmentation of pasta rod after instability development as observed in experiments (black) and NVE simulations (blue) (time $t/\tau = 0.85$). (Wood rod: $\tau = 2 \times 10^{-4}$ s; pasta rod: $\tau = 3.4 \times 10^{-4}$ s).

mode coarsening: rather than transferring energy from higher wave numbers to lower ones, the energy is dissipated in the formation of fractures [Fig. 3(b)].

We proceed by developing a quantitative theoretical framework that explains the experimentally observed mode coarsening in the dynamic postbuckling behavior of thin elastic rods. We place ourselves within the classical framework of dynamic Euler buckling of a beam (length ℓ, cross section A, moment of geometric inertia I, mass density ρ, Young's modulus E), subject to a compressive force P (e.g., [2]):

$$\rho A\ddot{\xi} + \frac{\partial^2}{\partial x^2}(EI\xi'') + \frac{\partial}{\partial x}(P\xi') = 0, \tag{1}$$

where $\xi = \xi(x,t)$ is the beam's lateral deflection. Our model departs from the assumption that the experimentally found energy transfer mechanism originates from a force relaxation mechanism. More specifically, if we equate the change in length, $\ell \simeq \int_0^{\ell-\delta\ell}(1+\frac{1}{2}\xi'^2)dx$, with the axial strain caused by the force, $P(k) = EA\epsilon$, for deflections of the form $\xi(x,t) \sim \xi_k \exp(ikx - i\omega t)$ along $x \in [0, \ell - \delta\ell]$, with $\xi_k \sim \xi_0 t_k/\tau$ the kth mode's lateral deflection magnitude, and $\delta\ell \approx U_0/c\ell$ the shortening induced by the impact of the projectile [11], whose velocity is U_0 (the speed of compressive waves is $c = \sqrt{E/\rho}$), we obtain a transient force relaxation of the form (see derivation in Supplemental Material [16]):

$$P(t < t_k) = P_0\left[1 - \left(\frac{t}{t_k}\right)^2\right] \quad \text{and} \quad t_k \sim \tau\frac{\sqrt{U_0/c}}{\xi_0 k}, \tag{2}$$

where $\tau \sim d/U_0$ is the characteristic time of impact and P_0 is the initial buckling force.

Next, we inspect solutions of Eq. (1) with Eq. (2) for $t < t_k$ and $t > t_k$ [when $P(t > t_k) = 0$] while ensuring continuity at $t = t_k$, and find (see Supplemental Material [16]):

$$\xi_k(t) = \xi_0 \cos(\omega_k t) + \frac{kd\sqrt{U_0 c}}{\omega_k}\sin(\omega_k t), \tag{3}$$

where $\omega_k = cdk^2$. Finally, with a focus on identifying a relation between the apparent dominant deflection wave number k at time t, we seek the maximum magnitude of the transient shape, from $\partial\xi_k/\partial k = cdt(\sqrt{U_0/c} - 2k^3 cdt\xi_0) + O(k^4) = 0$, and finally obtain the sought time-wave number scaling relation:

$$k = \left(\frac{U_0}{c}\right)^{1/6}\left(\frac{d}{c\xi_0}\right)^{1/3} t^{-1/3}. \tag{4}$$

Thus, as time t increases the wave number k, at which ξ_k reaches a maximum decreases. This is a hallmark of a mode coarsening mechanism induced by a pure geometric force relaxation process, as captured by Eq. (2). The decay, $k \sim t^{-1/3}$, is similar to the coarsening law observed in a wide variety of diffusive systems [18], though in the present case the process is purely inertial. The power scaling $k \sim t^{-a}$ is consistent with the experimental trends shown in Fig. 3(a). Still, the exponent obtained by fitting the experimental data is different; $k_{\text{exp}} \sim t^{-1/1.9}$ versus $k \sim t^{-1/3}$. This difference means that the experimental mode coarsening mechanism occurs faster in time than predicted by the model suggesting that the energy transfer from high to lower wave numbers is accelerated by some form of energy dissipation. While viscous material dissipation mechanisms can be excluded (given the extreme short duration of the buckling experiment), we remind ourselves that the experiment did not take place in vacuum, but in air involving losses due to the drag of the deforming rod with the surrounding air, a phenomenon known to influence coarsening dynamics [7,13].

To probe this hypothesis, we turn to molecular dynamics inspired structural simulations, and discretize the rod into mass points with interactions described by harmonic potentials of mean force suitable for structural members

for both two-body (stretch) and three-body (bending) interactions [7,19] (potential parameters are given in Supplemental Material [16], which includes Ref. [20]). We simulate the dynamic buckling test in two thermodynamic ensembles: the microcanonical ensemble (NVE), and the canonical ensemble (NVT) using a Nosé-Hoover thermostat [21,22]. The thermostat adds or removes heat in order to control temperature T. We load the rod by applying a linear strain ramp, $\delta\ell/\ell = (U_0/c)(t/t_0)H(1-t/t_0)$ at the free end [with $H(x)$ the Heaviside function], similarly to how the projectile impacts and shortens the beam. For $t > t_0$, we inspect the postbuckling behavior and follow the PSD evolution in time of the simulated lateral deflection.

Simulation results replicating the NVE ensemble are presented in Figs. 2(a) and 2(b), and NVT results along with experimental observations in Figs. 2(c) and 2(d) showing the PSD for a selected number of rod profiles at different times. In Fig. 3(a), we display the time-wave number scaling; that is, the time at which a specific wave number exhibits a maximum, obtained in an identical fashion of our analyses of the experimental results. First, the NVE results (shown in blue color) in Fig. 3(a) follow exactly the $k \sim t^{-1/3}$ scaling, which provides an *a posteriori* validation of our analytical force relaxation model [Eq. (4)]. Second, the NVT simulation results are in a very good agreement with the experimental results in both the PSD [Fig. 2(c)] and the instability growth [Fig. 2(d)]; but as well in terms of the time-wave number scaling (shown in black color) in Fig. 3(a), $k_{\mathrm{NVT}} \sim t^{-1/2}$ versus $k_{\mathrm{exp}} \sim t^{-1/1.9}$. All this provides strong evidence that the mode coarsening found in our experiments is affected by dissipation related to kinetic energy exchanges between the rod and the air represented in the NVT simulation by a thermalized bath.

We also obtain an excellent agreement between experiment and simulation of the brittle rod in terms of fragmentation [Fig. 3(b)], when considering cutoff stretch and rotations at which the bonds break (for parameters, see Supplemental Material [16]). Because of the very short time to fracture [$t/\tau < 1$, Fig. 1(c2)], there is no difference between NVE and NVT simulations. The absence of mode coarsening in dynamic buckling of brittle rods is thus due to the fact that neither energy transfer from higher to lower modes nor energy exchange with the bath suffice to reduce the strain energy in the rod to a level below the fracture energy of the material. Instead, the strain energy is dissipated in the formation of fractures.

A last point of inquiry we here address is the relevance of thermalization in the postbuckling behavior. For one, the observed mode coarsening involves energy transfer between instability modes far beyond the first static Euler buckling load, $P \gg P_{\mathrm{crit}} = \pi^2 EI/\ell^2$, with elastic instabilities that—by definition—do not represent equilibrium states. For the NVT simulations, it is thus of interest to find out how far the thermostat is able during instability growth and mode coarsening to control the temperature.

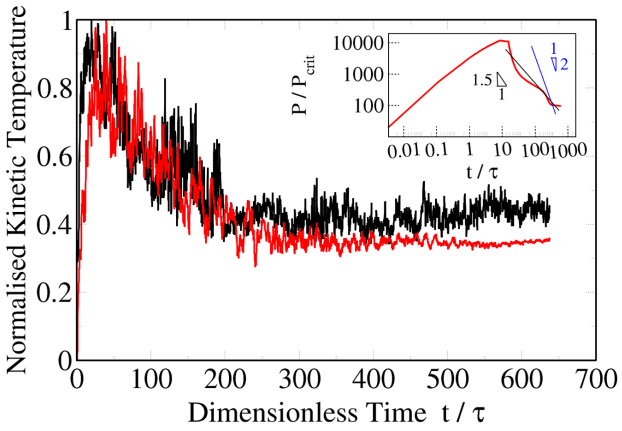

FIG. 4. Time evolution of normalized kinetic temperature, $E_{\mathrm{kin}}/\max E_{\mathrm{kin}}$, obtained from experimental observations (black) and NVT simulations. Noteworthy is the fact that the kinetic temperature does not decay to the prescribed bath temperature, $T_0 \to 0$. The inset shows the force relaxation obtained from NVT simulations. (Time t is normalized by the impact time $\tau = 2 \times 10^{-4}$ s; force P is normalized by the first static Euler buckling load, $P_{\mathrm{crit}} = \pi^2 EI/\ell^2$).

This is achieved here by introducing the kinetic temperature of the rod, $k_B T = (2/D)\bar{E}_k$, with k_B the Boltzmann constant, D the system's dimension, $\bar{E}_k = \langle \frac{1}{2} m_i \vec{V}_i \cdot \vec{V}_i \rangle$ the mean kinetic energy of N mass points of mass m_i and velocity $\vec{V}_i$. The evolution of the rod's kinetic temperature [Fig. 4] is determined from the lateral deflection rate, $V_i = \partial \xi_i/\partial t$, for both the experiment and the NVT simulation. Following a kinetic temperature burst in the early stages of instability growth, the kinetic temperature decays during mode coarsening, and reaches a horizontal asymptote. Moreover, we observe an overall force relaxation during this kinetic temperature decay, which is not far off the quadratic scaling with time as considered in our model [compare inset of Fig. 4 with Eq. (2)]. Noteworthy is the fact that the asymptotic value of the structure's kinetic temperature is well above the bath's temperature $T_0 \to 0$, prescribed in the simulations. This observation is readily attributed to the instability in dynamic buckling [23]: evoking the zeroth law (two systems are in equilibrium when they have the same temperature), it becomes apparent that the rod is not in thermodynamic equilibrium with the bath when the structure exhibits instabilities.

In summary, considering a fundamental question in the dynamics of elastic beams, curiously never explicitly addressed before, we have uncovered a new postbuckling mechanism, called mode coarsening, which has features of an inverse cascade-type transfer of energy, a novel insight in the physics of fragmentation. Our study shows that if an impacted rod has not broken during its first buckling response stage, it is unlikely that it will subsequently. In our (deterministic) theory, the deflection slope $k(t)\xi_k(t)$ of the most amplified wave number $k(t)$ with amplitude $\xi_k(t)$

in Eqs. (3) and (4), decays initially, and never exceeds its initial value. Of course, other ingredients like fracture delay, damage, defects (see, e.g., [24,25] and the review in [26]) are out of this description, and in some particular situations breakup may occur after coarsening has started. But within our theory it does not, consistent with our observations with brittle pasta.

The proposed model was validated through experiments and MD-inspired structural simulations in different thermodynamic ensembles, thus opening new venues toward safe design of engineering structures subject to impact-induced risk of buckling, ranging from skyscrapers, to aerospace structures and vehicle's crashworthiness, to name a few.

Research carried out by the Concrete Sustainability Hub (CSHub@MIT), with funding provided by the Portland Cement Association (PCA) and the Ready Mixed Concrete Research & Education Foundation (RMC E&F). Additional support was provided by the joint MIT-CNRS research unit enabling the sabbatical of EV at MIT; and by NSF Grant No. 1826122 for M. J. A. Q. All simulations were carried out with the open source code LAMMPS, distributed by Sandia National Laboratories, a U.S. Department of Energy laboratory [27].

*Corresponding author.
ulm@mit.edu

[1] W. Gautschi, SIAM Rev. **50**, 3 (2008).
[2] Z. Bažant and L. Cedolin, *Stability of Structures. Elastic, Inelastic, Fracture and Damage Theories* (World Scientific, Singapore, 2010).
[3] W. K. Chen, *Stability Design of Steel Frames* (CRC Press, Boca Raton, FL, 2018).
[4] K. K. Shukla, Y. Nath, E. Kreuzer, and K. V. Kumar, J. Aerosp. Eng. **18**, 215 (2005).
[5] M. Soheilypour, M. Peyro, S. J. Peter, and M. R. K. Mofrad, Biophys J. **108**, 1718 (2015).
[6] B. Budiansky and J. W. Hutchinson, in *Applied Mechanics*, edited by H. Görtler (Springer, Berlin, Heidelberg, 1966).
[7] L. Golubovic, D. Moldovan, and A. Peredera, Phys. Rev. Lett. **81**, 3387 (1998).
[8] W. J. Stronge, *Impact Mechanics* (Cambridge University Press, Cambridge, England, 2004).
[9] R. Vermorel, N. Vandenberghe, and E. Villermaux, Proc. R. Soc. A **463**, 641 (2007).
[10] F. Box, O. Kodio, D. O'Kiely, V. Cantelli, A. Goriely, and D. Vella, Phys. Rev. Lett. **124**, 198003 (2020).
[11] J. R. Gladden, N. Z. Handzy, A. Belmonte, and E. Villermaux, Phys. Rev. Lett. **94**, 035503 (2005).
[12] R. Vermorel, N. Vandenberghe, and E. Villermaux, Proc. R. Soc. A. **465**, 823 (2008).
[13] F. Box, D. O'Kiely, O. Kodio, M. Inizan, A. A. Castrejon-Pita, and D. Vella, Proc. Natl. Acad. Sci. U.S.A. **116**, 20875 (2019).
[14] K. Baczinsky, R. Lipowsky, and J. Kierfeld, Phys. Rev. E **76**, 061914 (2007).
[15] S. Moulinet and M. Adda-Bedia, Phys. Rev. Lett. **115**, 184301 (2015).
[16] See Supplemental Material at http://link.aps.org/supplemental/10.1103/PhysRevLett.126.045501 for (1) details about the experimental setup and the repeatability of the experiments; (2) the derivation of the force relaxation relation during dynamic postbuckling; (3) the postbuckling solutions with a transient force relaxation; and (4) additional information about the MD-inspired structural simulations.
[17] R. Kraichnan, Phys. Fluids **10**, 1417 (1967).
[18] I. M. Lifshitz and V. V. Slyozov, J. Phys. Chem. Solids **19**, 35 (1961).
[19] K. Keremides, M. J. Abdolhosseini Qomi, R. J. M. Pellenq, and F-J. Ulm, J. Eng. Mech. **144**, 04018066 (2018).
[20] H. Laubie, F. Radjai, R. Pellenq, and F.-J. Ulm, J. Mech. Phys. Solids **105**, 116 (2017).
[21] S. Nosé, J. Chem. Phys. **81**, 511 (1984).
[22] W. G. Hoover, Phys. Rev. A **31**, 1695 (1985).
[23] A. Louhghalam, R. J. M. Pellenq, and F-J. Ulm, J. Appl. Mech. **85**, 081001 (2018).
[24] M. de Buffon, Expériences sur la force du bois (second mémoire), in Mémoires de l'Académie Royale (Académie Royale des Sciences, Paris, 1741), pp. 292–334.
[25] S. M. Wiederhorn and L. H. Bolz, J. Am. Ceram. Soc. **53**, 543 (1970).
[26] E. Villermaux, Int. J. Fract. **206**, 171 (2017).
[27] S. Plimpton, J. Comput. Phys. **117**, 1 (1995).